Journal of Radioanalytical and Nuclear Chemistry (2018) 318:1931–1938
https://doi.org/10.1007/s10967-018-6265-7

Estimation of soil characteristics based on the depth distributions of ^{238}U, ^{232}Th, ^{226}Ra, ^{40}K activity concentrations using laboratory HPGe gamma spectrometry

Truong Thi Hong Loan[1,2] · Vu Ngoc Ba[1] · Nguyen Quang Đao[2] · Nguyen Ngoc Anh[2] · Mai Thanh Man[2] · Truong Huu Ngan Thy[1] · Huynh Thi Yen Hong[1] · Nguyen Van Thang[1] · Truong Minh Hoang[3]

Received: 25 June 2018 / Published online: 22 October 2018

Abstract
Identification of clay minerals and depositional environment in soil at Ben Tre Province—South Vietnam was studied in this work by using laboratory HPGe gamma spectrometry through the evaluation of ^{232}Th, ^{238}U, ^{226}Ra and ^{40}K natural radionuclide distributions in soil versus depths. The calculated values of activity concentration ranged from 2.13 ± 0.13 to 6.64 ± 0.40 ppm for ^{238}U, from 1.97 ± 0.12 to 4.95 ± 0.30 ppm for ^{226}Ra, from 8.87 ± 0.53 to 21.30 ± 1.27 ppm for ^{232}Th and from 0.85 ± 0.05 to $2.01 \pm 0.12\%$ for ^{40}K. The results showed that clay minerals at the investigated site can be divided into two major groups: montmorillonite (the Th/K ratio from 6.61 to 10.47) and kaolinite (from 12.37 to 19.79) which are in accordant with the previous studies at the investigated area.

Keywords Clay mineral · HPGe gamma spectrometry · Natural radionuclide · Th/K ratio

Introduction

Concentrations of uranium (U), thorium (Th) and potassium (K) in the geological materials provide many important lithological characteristics, database of geologic processes and sometimes ore deposit data information. The isotopes initially found mainly in acidic igneous rocks are usually transported due to geological processes to sediments where they usually accumulate in clay substance [1].

The important structural and chemical differences among the clay minerals are the basis for names of the individual mineral species and the arrangement of the species in groups. Clay minerals can be divided into four major groups including the kaolinite groups, montmorillonite groups (smectite), illite groups, chlorite groups: the kaolinite is clay mineral, with the chemical composition $Al_2Si_2O_5(OH)_4$. The kaolinite is being a widespread component of clay, where it is the result of weathering processes of feldspar. Rarely, it is the result of low-temperature hydrothermal processes. The montmorillonite—a very soft phyllosilicate group of minerals—is formed by its precipitate from water solution as microscopic crystals, known as clay with the chemical composition: (Na,Ca H)(Al,Mg,Fe,Zn)$_2$(Si,Al)$_4$O$_{10}$(OH)$_2$·nH$_2$O. The illite is non-expanding clay crystalline mineral. The chemical formula is given as (K,H$_3$O)(Al,Mg,Fe)$_2$(Si,Al)$_4$O$_{10}$[(OH)$_2$,(H$_2$O)]. The illite occurs as an altered product of muscovite and feldspar in weathering and hydrothermal environments. Finally, the chlorite is relatively large and not necessarily considered as clay. The chlorite minerals have a generalized chemical composition of (Fe,Mg,Mn,Ni,Zn,Ti)$_{4-6}$(Si,Al)$_4$O$_{10}$(OH,O)$_8$. The chlorite minerals most often form in rock environments where minerals are altered by heat, pressure, and chemical activity [2, 3].

There are many methods and technologies to determine activity concentration of natural radionuclides in clay core:

✉ Truong Thi Hong Loan
tthloan@hcmus.edu.vn

[1] Nuclear Technique Laboratory, VNUHCM University of Science, Linh Trung Ward, Thu Duc District, Ho Chi Minh City, Vietnam

[2] Faculty of Physics and Engineering Physics, VNUHCM University of Science, 227 Nguyen Van Cu Street, District 5, Ho Chi Minh City, Vietnam

[3] Department of Engineering Geology – Environmental Geology, VNUHCM University of Science, 227 Nguyen Van Cu Street, District 5, Ho Chi Minh City, Vietnam

Hesselbo [4] and Rahman [5] used spectral gamma ray logs methods, Fabricius et al. [6] used laboratory and borehole measurements, Malczewski et al. [7] carried out the assessment of radionuclides in rock and soil by in situ gamma ray spectrometry.

For the past century, natural radionuclide studies have been used for variety of applications in life. Freitas [8], Spadoni [9] conducted a study on characteristic distribution of natural radionuclides at the sand beach and floodplain sediment area. Uddin [2], Omoniyi [10] used gamma ray spectrometry to find rare metals. Hesselbo [4] and Fabricius et al. [6] used gamma ray for evaluation of siliciclastic sediments. Klaja and Dudek [11] determined the clay types based on the Th/K ratio.

Clay minerals are the most important component in minerals industries. Clay belongs to a wide mineral group, which has the capacity to hold metal (Au, Al, Ca, Mg, Mn, Fe, Zn, Cu, Na, K, Eu). Clays have been created for selective removal and recovery of heavy metals [12]. The montmorillonite K10 is utilized in a novel aryl migration from silicon to carbon or as a food additive for health and stamina [13]. Clays have been used for variety of applications especially in medical science, material science, industrial engineering and agriculture as an acidic and green catalysts for effective esterification of phenols and alcohols [14].

In this work, the geological structure at Ben Tre, South Vietnam was studied by radioactivity analysis method using gamma spectrometry with laboratory HPGe detector. The natural radionuclides are used as tracers of the mineralogical properties. It involves (1) the study on depth distribution of ^{238}U, ^{232}Th and ^{40}K radionuclides in clays from which geological structure were estimated; (2) the determination of the Th/K ratio which related to the types of clay minerals.

Materials and methods

The investigated site and sample collection

The Mekong River begins from the mountainous area of Tibet and ends at a wide delta in Vietnam, one of the largest deltas in Asia. It is 4350 km long, with a drainage area of 810,000 km^2.

Ben Tre is a province of Mekong Delta. It is 87 km from Ho Chi Minh City in the western. The South pole is located at latitude *9°48′* North, the North pole is at latitude *10°20′* North, the East pole is at *106°48′* East and the West pole is at *105°57′* East.

Ben Tre Province consists of a broad coastal plain corresponding to the lower northeastern part of the delta plain, located among the active distributaries of the Mekong River system (Fig. 1). Geographically, Ben Tre is wedged between the two main branches of the Mekong River. The weather in Ben Tre is typically monsoon tropical with high average temperatures of 26–27 °C. The rainy season usually are from May to October.

The clay samples were collected at Quarter 4, Chau Thanh Town, Chau Thanh District, Ben Tre Province. The samples were taken by thin steel tube sampler with a length of 70 cm and a diameter of 110 mm using hydraulic compression. The soil samples were taken to 40 m in depth. The soil core was then sectioned into 2 m increments which are used for analyzed sample preparation. Collected samples were labeled and wrapped with paraffin (Fig. 2).

The soil samples were transported to the laboratory, dried at room temperature, crushed to their particle sizes of less than 0.2 mm. Then samples were dried at 105 °C for 8 h and packed in a cylinder of 76.6 mm diameter and 20 mm height. The soil samples were sealed within 30 days in order to reach secular equilibrium between ^{226}Ra radionuclide and its daughters in uranium series.

Measurements and analysis

Activity concentrations of natural radionuclides in the samples were determined using a n-type coaxial detector of GMX35P470 from Ortec having its relative efficiency of 35%, its energy resolutions of 1.8 keV at the 1332.5 keV energy of ^{60}Co, of 1.02 keV at the 122.06 keV energy of ^{57}Co. The soil samples were acquired for a enough long time (about 86,400 s) to achieve the statistical error of counting of less than 1%.

Among the radionuclides belonging to a natural decay series, ^{238}U cannot be directly measured by gamma spectrometry but only via its daughter radionuclides of ^{234}Th (63.38 keV) and ^{234m}Pa (1001 keV), in which 63.38 keV of ^{234}Th is often used. The ^{226}Ra activity concentration was estimated from ^{214}Pb (295.2 keV and 351.9 keV) and ^{214}Bi (609.3 keV) for sample assumed to be in secular equilibrium. ^{232}Th can be determined through isotopes ^{228}Ac (338.3 keV, 911.2 keV), ^{212}Pb (238.6 keV) and ^{208}Tl (583.2 keV, 2614.3 keV). The activity concentration of ^{40}K was determined directly by its own gamma ray 1460.83 keV [15].

The activity concentrations of radionuclides in the measured samples (A) were calculated using the following equation:

$$A = \frac{N}{\varepsilon(E) \times f \times m \times t \times K_c \times K_w} \quad (1)$$

where A is the sample activity concentration on the sampling date (Bq/kg), N is the net peak area, ε(E) is full energy peak efficiency (FEPE) of detector, f is the branching ratio of the E gamma energy under

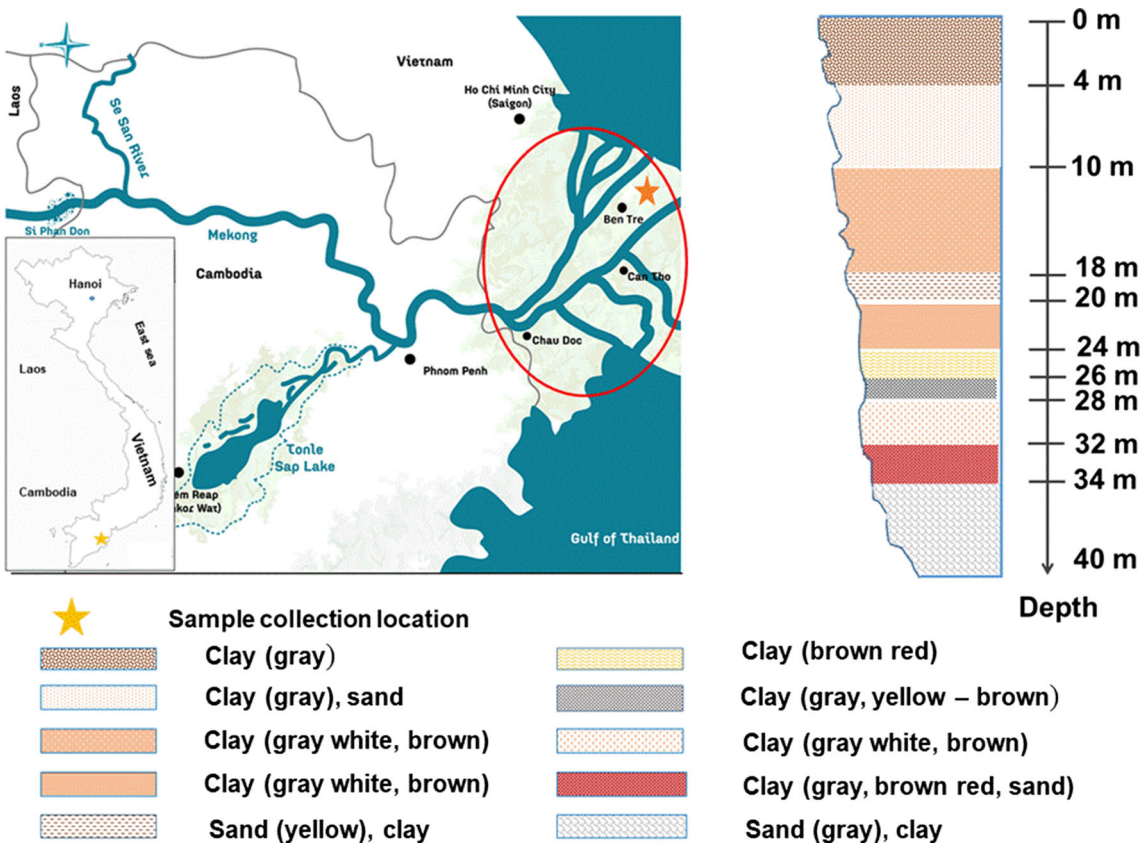

Fig. 1 Map of sampling in Ben Tre Province

Fig. 2 Soil cores taken from the steel tube sampler

consideration, m is the mass of the sample (kg) and t is the collection live time (s), K_c is the correction factor for the nuclide decay during counting and K_w is the correction factor for the nuclide decay from the time the sample was obtained to the start of acquisition.

The minimum detection activity MDA (Bq/kg) values were also calculated for every interested energy line by Eq. (2).

$$\mathrm{MDA} = \frac{L_D}{\varepsilon(E) \times f \times m \times t \times K_c \times K_w} \tag{2}$$

where $L_D = 2.71 + 4.66\sqrt{B}$ is detection limit for confidence interval of 95%; B is calculated continuum under the peak [16].

FEPE values at different gamma energies for analysis samples were calibrated by using Angle 3.0 (Ortec) [17]. This method combines the measured efficiency of a reference configuration and solid angle model to derive the efficiency for different sample containers, materials, and densities. The FEPEs were also corrected by summing coincidence factor using TrueCoinc software for multi gamma emitted radioisotopes [18]. In this work, reference source of RGU1 which is contained in the cylinder beaker of a 7.66 cm in diameter and a 2 cm in height [19].

The standard uncertainty of activity is calculated by equation:

$$\frac{\sigma_A^2}{A^2} = \frac{\sigma_N^2}{N^2} + \frac{\sigma_m^2}{m^2} + \frac{\sigma_f^2}{f^2} + \frac{\sigma_\varepsilon^2}{\varepsilon^2} \tag{3}$$

where σ_A^2 σ_N^2 σ_m^2 σ_f^2 σ_ε^2 are standard deviation of A, N, m, f and ε respectively.

Results and discussions

Validation of the analysis procedure using HPGe gamma spectrometer

The IAEA-TEL-2016 test samples of Sample 1, Sample 2 and IAEA standard samples of RGK1 and RGTh1 were analyzed by using gamma spectrometer with HPGe detector of GMX35P470 following setup procedure by our NTLab [19]. The RGU1 standard sample which was packed in the same cylinder geometry of a 7.66 cm in diameter and a 2 cm in height was used for calculating the experimental full energy peak efficiency (FEPE) named $FEPE_{ex}$. The $FEPE_{ex}$ was corrected by summing coincidence factor using TrueCoinc software for multi gamma emitted radioisotopes [18]. Angle 3.0 software of Ortec Industries Inc. was used to transfer the calculated $FEPE_{ex}$ in the FEPE for every analyzed sample and for each energy of interest. The chemical composition of DIRT 1 was used for RGU1, RGTh1, RGK1 samples and the analyzed soil samples [16], the chemical composition of H_2O was used for Sample 1, Sample 2. These data and the sample densities were used in Angle software to calculate FEPEs respectively. Table 1 presented the FEPE calculated from the measurement of RGU1 standard sample ($FEPE_{ex}$) and the FEPE corrected by the (COI) summing coincidence effect ($FEPE_{coi}$). FEPEs calculated by Angle for each energy and each analyzed sample were not illustrated in this paper. Table 2 showed a comparison between activity concentration from the analytical results with the reference values by the IAEA.

Table 1 The $FEPE_{ex}$ calculated from the measurement of the RGU1 standard sample and the $FEPE_{coi}$ corrected by the (COI) summing coincidence effect

E (keV)	$FEPE_{ex}$	COI	$FEPE_{coi}$
46.54	0.0486	1.000	0.0486
63.3	0.0675	1.000	0.0675
242.0	0.0442	1.041	0.0460
295.22	0.0381	0.995	0.0379
351.93	0.0331	1.001	0.0331
609.31	0.0173	1.146	0.0198
768.36	0.0160	1.185	0.0190
785.96	0.0159	1.158	0.0184
934.06	0.0128	1.171	0.0149
1120.3	0.0117	1.166	0.0136
1238.1	0.0109	1.157	0.0126
1377.7	0.0113	0.959	0.0108
1509.2	0.0094	1.132	0.0107
1764.5	0.0092	1.003	0.0092
2118.6	0.0082	0.919	0.0075
2204.2	0.0074	0.997	0.0074
2447.9	0.0068	0.987	0.0067

The relative deviations of calculated values compared with reference IAEA values are less than 5% for different radionuclides contained in four analyzed samples. Therefore the reliability of the used analysis method is ensured in measurement for soil samples.

The activity concentration distribution of ^{238}U, ^{226}Ra, ^{232}Th, ^{40}K versus depths

The depth distributions of the activity concentration and their ratio in clay were presented in Tables 3, 4 and demonstrated in Fig. 3. The values of activity concentration ranged from 2.13 ± 0.13 to 6.64 ± 0.40 ppm for ^{238}U, from 1.97 ± 0.12 to 4.95 ± 0.30 ppm for ^{226}Ra, from 8.87 ± 0.53 to 21.30 ± 1.27 ppm for ^{232}Th and from 0.85 ± 0.05 to $2.01 \pm 0.12\%$ for ^{40}K. The variations in activity concentration among the clay samples may be attributed to their radioactive mineral content and the geochemical and geographical origins of the clay, among other factors.

The estimated activity values were classified to identify soil layers at the investigated site. In details, activity concentration of less than 3 ppm is low, one from 3 to 6 ppm is moderate and one of more than 6 ppm is high for U and Th; and it is less than 1%, from 1 to 2%; more than 2% respectively for low, moderate and high activity for potassium [5, 20]. As results, all samples have high activity concentration in thorium. Meanwhile, the activity concentration ranged from low to moderate for uranium and potassium. However, it becomes high at the 32 m depth for potassium. Therefore, it is concluded that there is no carbonate or shaly carbonate with clay minerals, no organic matter, the oxidizing environment at the site. The high in Th/K ratios are associated with clay mineral suites dominated by kaolinite and/or smectite. The ratios of Th/U values from 2.91 ± 0.25 to 5.63 ± 0.48 proved that the types of clay minerals are grey, greywackes and green shales, the result is also found in the work of Klaja and Dudek [11].

Based on the radionuclide activity of thorium and uranium in Fig. 3, three different cores were identified: i; depth from 0 to 8 m, ii; depth from 10 to 34 m, iii; depth from 36 to 40 m. It is related to differences in chemical composition, soil structure and clay type. Similarities were found in the research of Bao et al. [21] who studied the changes of geotechnical properties of the sediment at Ben Tre. From Table 3 and Fig. 3e, the $^{226}Ra/^{238}U$ activity ratio of 0.86 in average, the activity concentration of ^{238}U was not equal to the one of its daughter products—^{226}Ra. It showed that secular equilibrium did not exist for almost the analyzed samples. Dostal and Capedri [22] have demonstrated that whole rock uranium content decreases with

Table 2 Comparison between activity concentration from the analytical results with the reference values by the IAEA

Sample	Radioisotope	Activity concentration (Bq/kg)		Ratio (1)/(2)
		Present work (1)	IAEA [18] (2)	
Sample 1	^{22}Na	50.55±0.77	53.20±1.50	0.95±0.03
	^{137}Cs	38.17±0.84	39.60±0.50	0.96±0.02
	^{134}Cs	20.45±0.44	19.90±1.00	1.03±0.06
Sample 2	^{241}Am	25.52±0.04	26.70±0.70	0.96±0.03
RGK1	^{40}K	13,630±136	14,000±400	0.97±0.03
RGTh1	^{232}Th	3190±160	3250±90	0.98±0.06

Table 3 The activity concentration distribution of natural radionuclides versus depths

Depth (m)	Activity concentration			
	^{238}U (ppm)	^{226}Ra (ppm)	^{40}K (%)	^{232} Th (ppm)
0	4.33±0.26	2.65±0.16	1.73±0.10	14.71±0.88
2	3.69±0.22	2.74±0.16	1.52±0.09	12.55±0.75
4	2.33±0.14	2.42±0.15	1.47±0.09	13.11±0.79
6	2.27±0.14	1.97±0.12	1.31±0.08	9.18±0.55
8	2.13±0.13	1.97±0.12	1.04±0.06	8.87±0.53
10	2.74±0.16	2.66±0.16	1.29±0.08	12.03±0.72
12	4.49±0.27	4.68±0.28	0.85±0.05	13.93±0.84
14	4.97±0.30	3.54±0.21	0.89±0.05	17.53±1.05
16	2.87±0.17	2.77±0.17	1.44±0.08	11.69±0.70
18	4.09±0.25	3.84±0.23	1.80±0.10	16.28±0.98
20	3.67±0.22	3.68±0.22	0.98±0.06	16.20±0.97
22	4.06±0.24	3.99±0.24	1.11±0.07	11.66±0.70
24	6.64±0.40	3.97±0.24	1.71±0.10	21.13±1.27
26	3.93±0.24	3.86±0.23	1.61±0.10	21.30±1.27
28	4.21±0.25	4.09±0.25	1.99±0.12	18.62±1.12
30	6.30±0.38	4.95±0.30	1.19±0.07	18.35±1.10
32	4.17±0.25	3.99±0.24	2.01±0.12	18.14±1.09
34	4.21±0.25	3.38±0.20	1.47±0.09	13.76±0.83
36	3.23±0.19	2.69±0.16	1.56±0.09	11.43±0.69
38	2.51±0.15	2.50±0.15	1.62±0.10	10.71±0.64
40	3.44±0.20	2.93±0.18	1.46±0.09	13.08±0.78
MDA	0.68	0.12	0.02	0.55

increasing grade of metamorphism such that only firmly bound uranium remains after granulite metamorphism. Although the geochemistry of the radioisotopes, together with clay physicochemical information may give clues on the profile patterns and on the radio Ra/U [21, 23]. Further investigations are needed to comprehensively characterize the geological structure under study.

Table 4 The distribution of activity concentration ratio versus depths

Depth (m)	^{232}Th/^{40}K	^{232}Th/^{238}U	^{226}Ra/^{238}U
0	8.50±0.71	3.40±0.29	0.61±0.05
2	8.26±0.69	3.40±0.29	0.74±0.06
4	8.92±0.77	5.63±0.48	1.04±0.09
6	7.01±0.60	4.04±0.35	0.87±0.08
8	8.53±0.71	4.16±0.36	0.92±0.08
10	9.33±0.80	4.39±0.37	0.97±0.08
12	16.39±1.38	3.10±0.26	1.04±0.09
14	19.70±1.62	3.53±0.30	0.71±0.06
16	8.12±0.66	4.07±0.34	0.97±0.08
18	9.04±0.74	3.98±0.34	0.94±0.08
20	16.53±1.42	4.41±0.37	1.00±0.08
22	10.50±0.91	2.87±0.24	0.98±0.08
24	12.36±1.04	3.18±0.27	0.60±0.05
26	13.23±1.14	5.42±0.46	0.98±0.08
28	9.36±0.80	4.42±0.37	0.97±0.08
30	15.42±1.30	2.91±0.25	0.79±0.07
32	9.02±0.76	4.35±0.37	0.96±0.08
34	9.36±0.80	3.27±0.28	0.80±0.07
36	7.33±0.61	3.54±0.30	0.83±0.07
38	6.61±0.57	4.27±0.36	1.00±0.08
40	8.96±0.77	3.80±0.32	0.85±0.07

Determination of clay mineral types

The function of the metal elements depends on the clay types [2, 24], therefore, it takes an account of the clay types researched. Many authors have used these methods and techniques for studying clay and improving the means for the direct study of finely crystalline materials like the clays. In this work, determinations of the types of clay minerals are carried out on the basis of empirical relationships of the thorium to potassium ratios. The values of Th/K ratio are different for different minerals. For example, Feldspars:< 0.6; Glauconite: 0.6–1.5; Micas: 1.5–2.0; Illite: 2.0–3.5; Montmorillonite: 3.5–12.0; Kaolinite: 12.0–25.0; Heavy thorium–bearing minerals:>25.0) [5, 11]. Figure 4 showed

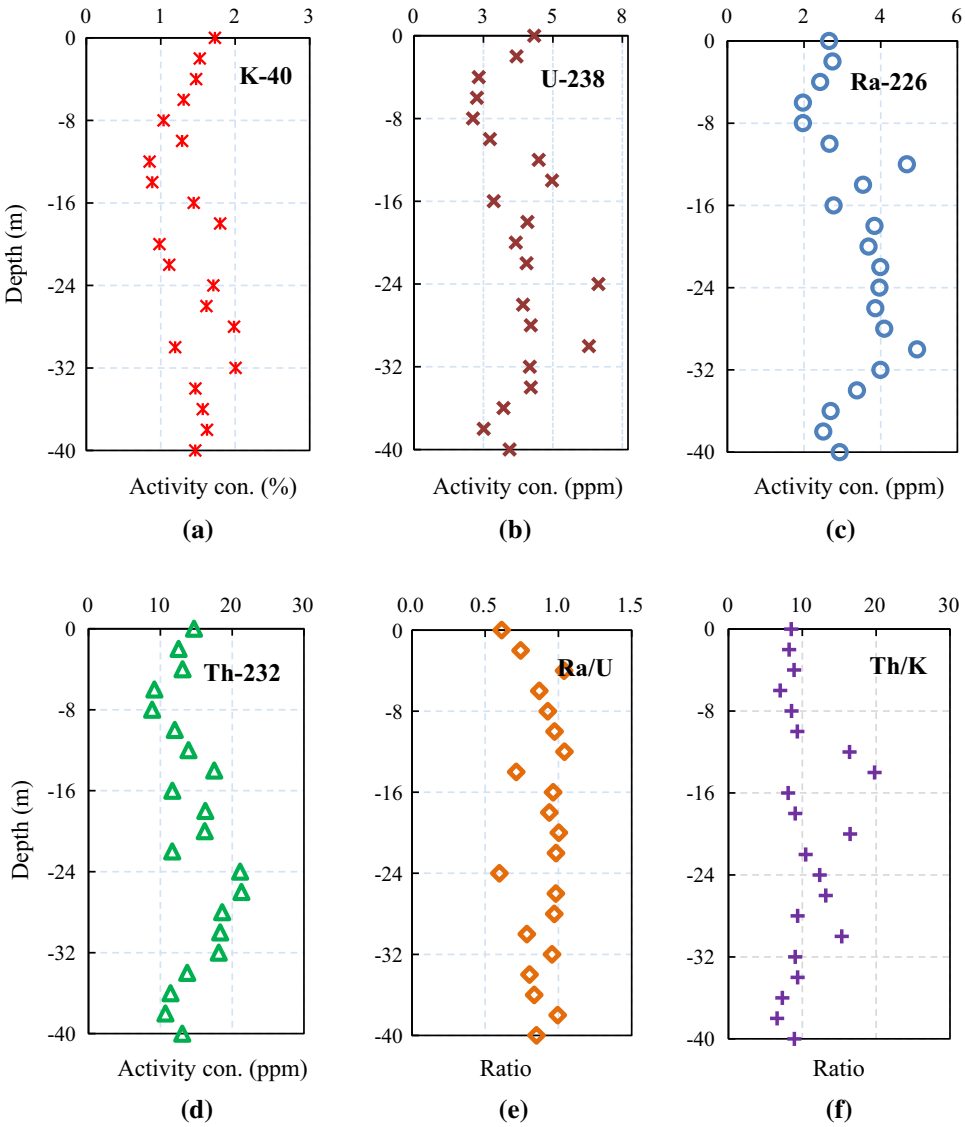

Fig. 3 The depth distribution of the activity concentrations of the natural radionuclides and their ratios at the investigating site

the crossplot of the Th/K ratio for mineral identification using spectral gamma ray data for 21 samples of soils taken at depths from 0 to 40 m at the investigated site. The results showed that two main types of clays are kaolinite and montmorillonite. Six samples which are in position from 12 to 14 m, 20 m, from 24 to 26 m and 30 m belong to kaolinite. So it is accounted for 28.6% in total. The remaining clay is mainly montmorillonite.

Comparisons with the same area: Ta et al. [23], Le [25] have published their extensive studies in the sediment of the Mekong Delta. Results also showed that the sediment in the Mekong Delta contains the main clay mineral as hydromica, kaolinite, montmorillonite and chlorite. Shinji et al. [26] proved that the class alluvial deposition is the main component of hydromica and kaolinite, but the amount of smectite tends to increases with the depth of the sediment. Phạm and Bùi [27] who studied sediments from the surface to 15 m in depth also found that the decrease of hydromica, montmorillonite and two minerals account for more than 60–70%. Therefore analysis methods for sediment using radioactive techniques in this work give reliable results. It is a facility to help us identify subsurface structure and maps in archaeological, geotechnical or faults related to abnormal radioactive as studied by Fabricius et al.; Hesselbo [4, 7].

Conclusion

This work has demonstrated the usefulness of gamma ray spectrometry studies in identification of soil structure, characteristics of Ben Tre coast using natural radionuclides of ^{232}Th, ^{238}U, ^{226}Ra. These radionuclides and their ratio as Th/K ratio are effectively used as tracers of the geological

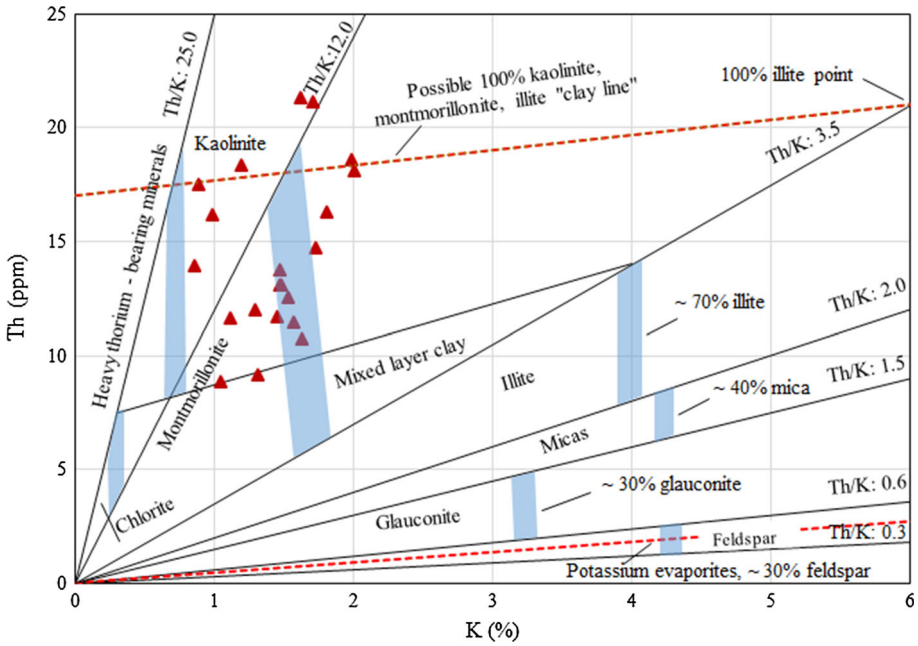

Fig. 4 Clay mineral types determined from the activity concentration of thorium (ppm) and potassium (%)

provenance to evaluate the types of clay minerals and the characteristics of sedimentary conditions.

Results showed that clays at investigating area can be divided into the kaolinite and montmorillonite, through which we can predict mineral potential, the origin of geological formation in the study area formation or the use in architecture, industry, and agriculture. The radioactive analysis method can be well applied for studying sedimentary origin, soil structure or finding some features of clay mineral distribution.

Acknowledgements We express our sincere thanks to: Vietnam National University—Ho Chi Minh City for supporting the HPGe detectors for our NTLab. The editor in chief and the reviewers for improving the overall quality of the paper.

References

1. Constable JL, Hubbard FH (1981) U, Th, and K distribution in a differentiated charnockite—granite intrusion and associated rocks from SW Sweden. Mineral Mag 44:409–415
2. Uddin F (2008) Clays, nanoclays, and montmorillonite minerals. Metall Mater Trans A 39:2804–2814
3. Al-Ani T, Sarapää O (2008) Clay and clay mineralogy. Physical–chemical properties and industrial uses. Geological Survey of Finland, GTK Publisher, pp 3–4
4. Hesselbo SP (1996) Spectral gamma-ray logs in relation to clay mineralogy and sequence stratigraphy, Cenozoic of the Atlantic margin, offshore New Jersey. In: Proceedings of the Ocean Drilling Program, scientific results, vol 150, pp 411–422
5. Rahman AYAA (2013) Clay Lithofacies and depositional environment, as deduced from natural gamma-ray spectroscopy and petrographical data of the Abu Roash "E" member, GPT field, Western Desert, Egypt. Middle East J Sci Res 16(8):1027–1036
6. Fabricius IL, Fazladic LD, Steinholm A, Korsbech U (2003) The use of spectral natural gamma-ray analysis in reservoir evaluation of siliciclastic sediments: a case study from the Middle Jurassic of the Harald Field, Danish Central Graben. Geol Surv Den Greenl Bull 1:349–366
7. Malczewski D, Teper L, Dorda J (2004) Assessment of natural and anthropogenic radioactivity levels in rocks and soils in the environs of Swieradow Zdroj in Sudetes, Poland, by in situ gamma-ray spectrometry. J Environ Radioact 73(3):233–245
8. Freitas AC, Alencar AS (2004) Gamma dose rates and distribution of natural radionuclides in sand beaches—Ilha Grande, SouthEastern Brazil. J Environ Radioact 75(2):211–223
9. Spadoni M, Voltaggio M (2013) Contribution of gamma ground spectrometry to the textural characterization and mapping of floodplain sediments. J Geochem Explor 125:20–33
10. Omoniyi IM, Oludare SMB, Oluwaseyi OM (2013) Determination of radionuclides and elemental composition of clay soils by gamma-and X ray spectrometry. Springerplus. https://doi.org/10.1186/2193-1801-2-74
11. Klaja J, Dudek L (2016) Geological interpretation of spectral gamma ray (SGR) logging in selected boreholes. Nafta Gaz. https://doi.org/10.18668/ng2016.01.01
12. Malakul P, Srinivasan KR, Wang HY (1998) Metal adsorption and desorption characteristics of surfactant-modified clay complexes. Ind Eng Chem Res 37(11):4296–4301
13. Nasreen A (2001) Montmorillonite. Synlett 2001(8):1341–1342
14. Marvi O, Fekri LZ, Takhti M (2014) Montmorillonite K10 and KSF clays as acidic and green catalysts for effective esterification of phenols and alcohols under MWI. Russ J Gen Chem 84 (9):1837–1840
15. British Standard (2005) Measurement of radioactivity in the environment—Soil. BS ISO 18589 - 1: 2005
16. Canberra Industries (2004) Genie 2000 version 30—customization tools manual. Canberra Industries Inc., Meriden
17. Industries O (2012) Angle 3 software of semiconductor detector efficiency calculation. Ortec Industries, Patna
18. Vidmar T (2010) True coincidence summing corrections CCCC, a deterministic code. Jozef Stefan Institute, Ljubljana

19. IAEA (2018) Reference materials/interlaboratory comparisons, cited at 21 August, 2018. https://nucleus.iaea.org/rpst/ReferenceProducts/Proficiency_Tests/index.htm
20. Ehrenberg SN, Svănă TA (2001) Use of spectral gamma-ray signature to interpret stratigraphic surfaces in carbonate strata: an example from the Finnmark carbonate platform (Carboniferous–Permian), Barents Sea. AAPG Bull 85(2):295–308
21. Bao TT, Hoang TM, Oanh TTK, Van Lap N (2015) Changes of geotechnical properties of the Holocene sediments at Giong Trom-Ben Tre. J Sci Technol Dev 18(6):102–113
22. Dostal J, Capedri S (1978) Uranium in metamorphic rock. Contrib Mineral Petrol 66(4):409–414
23. Ta TKO, Nguyen VL, Tateishi M, Kobayashi I, Saito Y, Nakamura T (2002) Sediment facies and Late Holocene progradation of the Mekong River Delta in Bentre Province, southern Vietnam: an example of evolution from a tide-dominated to a tide- and wave-dominated delta. Sediment Geol 152(3–4):313–325
24. Ross CS, Hendricks SB (1945) Minerals of the montmorillonite group. United States Department of the Interior, Washington, pp 23–79
25. Le XT (2005) Some features of distribution of clay minerals in the Mekong River Plain. Tạp chí Địa chất (J Geol) 295/7-8/2005
26. Shinji T, Sotham S, Sim I, Takebayashi H, Ooji A, Bunnarin B, Sambath T (2005) Lithological features of cored sediments from the southern part of lake Tonle Sap and Tonle Sap River, Cambodia. In: Proceedings of 1st international symposium on evaluation of mechanisms sustaining the biodiversity in Lake Tonle Sap, Phnom Penh
27. Phạm H, Bùi VT (1985) Những tài liệu mới về vùng sét Tây Nam sông Hậu TTBC hội nghị KHKT Địa chất lần thứ 2. Tổng cục Địa chất, Hà Nội 4:62–69